PHARMACOKINETIC DYNAMIC RELATIONSHIPS

Pharmacokinetic–pharmacodynamic modelling of acute N-terminal pro B-type natriuretic peptide after doxorubicin infusion in breast cancer

Shuang Liang[1]*, Richard C. Brundage[1], Pamala A. Jacobson[1], Anne Blaes[2] and Mark N. Kirstein[1,3]

[1]Department of Experimental and Clinical Pharmacology, College of Pharmacy, University of Minnesota, Minneapolis, MN 55455, USA, [2]Division of Hematology/Oncology/Transplantation, University of Minnesota, Minneapolis, MN 55455, USA and [3]Masonic Comprehensive Cancer Center, University of Minnesota, Minneapolis, MN 55455, USA

*Current address: Department of Metabolism and Pharmacokinetics, Bristol-Myers Squibb, Princeton, NJ, USA

AIMS
The aim of the present study was to develop a pharmacokinetic–pharmacodynamic (PK-PD) model to characterize the relationship between plasma doxorubicin and N-terminal pro B-type natriuretic peptide (NT-proBNP) concentrations within 48 h of doxorubicin treatment.

METHODS
The study enrolled 17 female patients with stages 1–3 breast cancer and receiving adjuvant doxorubicin (60 mg m^{-2}) and cyclophosphamide (600 mg m^{-2}) every 14 days for four cycles. In two consecutive cycles, plasma concentrations of doxorubicin, doxorubicinol, troponin and NT-proBNP were collected before infusion, and up to 48 h after the end of doxorubicin infusion. Nonlinear mixed-effects modelling was used to describe the PK-PD relationship of doxorubicin and NT-proBNP.

RESULTS
A three-compartment parent drug with a one-compartment metabolite model best described the PK of doxorubicin and doxorubicinol. Troponin concentrations remained similar to baseline. An indirect PD model with transit compartments best described the relationship of doxorubicin exposure and acute NT-proBNP response. Estimated PD parameters were associated with large between-subject variability (total assay variability 38.8–73.9%). Patient clinical factors, including the use of enalapril, were not observed to be significantly associated with doxorubicin PK or NT-proBNP PD variability.

CONCLUSION
The relationship between doxorubicin concentration and the acute NT-proBNP response was successfully described with a population PK-PD model. This model will serve as a valuable framework for future studies to identify clinical factors associated with the acute response to doxorubicin. Future studies are warranted to examine the relationship between this acute response and subsequent heart failure. Should such a relationship be established, this model could provide useful information on patients' susceptibility to doxorubicin-induced long-term cardiotoxicity.

WHAT IS ALREADY KNOWN ABOUT THIS SUBJECT

- Doxorubicin is a first-line cytotoxic agent used for treating patients with malignancies, including breast cancer. However, total lifetime doses, and thus efficacy, are capped to limit the associated cardiomyopathy and congestive heart failure.
- Despite limited total doses, cardiotoxicity can develop in 2–7% of patients months or even years after treatment, and angiotensin-converting enzyme (ACE) inhibitors are often prescribed to prevent and reduce severity.
- Early predictive markers of susceptibility are needed, so patients at greatest risk could be identified and personalized approaches to treatment developed.

WHAT THIS STUDY ADDS

- N-terminal pro-brain natriuretic peptide (NT-proBNP) and troponin are commonly measured cardiac biomarkers, and we observed that plasma NT-proBNP concentrations dramatically increased 24–48 h after doxoburicin infusion, but troponin did not.
- A population pharmacokinetic-pharmacodynamic model was developed to describe the relationship between doxorubicin exposure and the plasma acute NT-proBNP response.
- High (several-fold) between-patient variability was observed in patients' NT-proBNP acute responses. Even though ACE inhibitor treatment was not found to have a significant effect on NT-proBNP variability, we propose that the model can be used to test for the importance of other patient-specific covariates and would prove useful in predicting the acute NT-proBNP response.

Introduction

Doxorubicin is an integral component of treatment regimens for breast cancer, childhood solid tumours, soft tissue sarcomas and lymphomas. Most commonly, it is used in the treatment of breast cancer in the adjuvant and metastatic setting [1–3]. Although doxorubicin is highly effective in treating tumours, its therapeutic potential is greatly limited by its associated cardiotoxicity, including cardiomyopathy and congestive heart failure [4–6].

Doxorubicin is an anthracycline, containing aglycone tetracyclic and sugar moieties, and it intercalates into DNA strands and also inhibits topoisomerase II–DNA cleavage complexes. Once these complexes are trapped, DNA replication and transcription are blocked, resulting in tumour cell death. Multiple cellular mechanisms appear to be involved in doxorubicin-induced cardiotoxicity [6–9]. The most widely accepted hypothesis is iron-catalysed induction of cardiac oxidative stress. Other mechanisms include intracellular calcium dysregulation, impaired gene expression of various cardiac proteins [10], dysregulation of protein degradation by the ubiquitin–proteasome system [11], induction of mitochondrial DNA lesions [12], and targeting topoisomerase 2-beta [13] and mitochondrial topoisomerase [14]. The major metabolite of doxorubicin, doxorubicinol (doxo'ol) [15], is less potent than doxorubicin in its antitumour activity, although it may also contribute to the cardiotoxicity (reviewed in [16]).

The incidence and severity of doxorubicin-induced cardiotoxicity are dose dependent. The incidence rate sharply increases up to 30% after receiving cumulative doses above 550 mg m^{-2}; therefore, lifetime dose limits are used to minimize this risk [17–20]. However, 2–7% of patients will still develop cardiotoxicity, even if lifetime cumulative doses are below 550 mg m^{-2} [21]. Various strategies have been tried to ameliorate anthracycline-associated cardiotoxicity, including angiotensin-converting enzyme inhibitors (ACEIs) such as enalapril. It is not clear whether ACEI effects are direct or systemic (e.g. having an effect on arterial blood pressure) but they do not appear to impede anthracycline antitumour activity or affect pharmacokinetics (PK) [22, 23]. As the onset of doxorubicin-induced cardiotoxicity may not be evidenced

until years after the cessation of chemotherapy [7], it would be clinically beneficial if susceptible individuals could be identified during the early stages of chemotherapy.

Cardiac biomarkers such as N-terminal pro-brain natriuretic peptide (NT-proBNP) and troponin have been proposed as useful in evaluating anthracycline-induced myocardial injury [24–27]. NT-proBNP is a protein that is released in response to cardiac stress [28]. In the context of numerous triggers, most notably myocardial stretch (as occurs with ventricular overload) or an increase in wall tension, gene transcription in the cardiomyocyte is induced, resulting in an increase in the production of a hormone precursor named pre-proBNP. After several steps of molecular processing, NT-proBNP is generated and released from the cardiomyocyte. NT-proBNP is commonly used as a biomarker to evaluate the presence and severity of heart failure [28–30]. It has also been suggested that the magnitude and/or duration of acute response in NT-proBNP (i.e. 24 h after doxorubicin administration) correlated with left ventricular impairment 3–12 months after chemotherapy exposure [31, 32]. Therefore, understanding and characterizing the acute NT-proBNP response (e.g. the degree and rate of response), especially in relationship to chemotherapy agent exposure, may provide useful information that would enable better prediction of later cardiotoxic symptoms.

The aim of the current study was to develop a population PK–pharmacodynamic (PD) model to characterize the relationship between plasma doxorubicin and NT-proBNP concentrations within 48 h of doxorubicin treatment. Such a model will serve as a valuable tool in future studies to investigate the effects of patient characteristics that might affect PK and/or PD parameters.

Methods

Patient population/study design/analytical assay

The data for the current study were collected prospectively as part of a randomized clinical study to evaluate for possible

drug–drug interaction between doxorubicin and enalapril, an ACEI that is frequently used in the setting of anthracycline-induced cardiotoxicity. The study was approved by the Institutional Review Board and the Cancer Protocol Review Committee. Details of the primary study were described by Blaes *et al.* [22]. Briefly, the study recruited women over the age of 18 years with normal liver and kidney function with stages 1–3 breast cancer and receiving adjuvant doxorubicin (60 mg m^{-2}) and cyclophosphamide (600 mg m^{-2}) every 14 days for four cycles. In a crossover design, patients were randomly assigned to receive one cycle of chemotherapy with enalapril and another cycle without enalapril. The two study cycles were consecutive, and the sequence of enalapril cycle was assigned by randomization at study enrolment. During the cycle with enalapril, patients started enalapril therapy 7 days prior to the scheduled doxorubicin regimen at 5 mg per day for 4 days, and then increased to 10 mg per day for 3 days. PK studies were performed following doxorubicin administration on both cycles. Whole blood was collected into ethylenediamine tetraacetic acid tubes before infusion, and at 0.5 h, 1 h, 2 h, 4 h, 24 h and 48 h after the end of the doxorubicin infusion. Plasma was immediately isolated by centrifugation and frozen. Samples were stored at −80 °C until the time of analysis. Plasma doxorubicin and doxo'ol concentrations were measured by high-performance liquid chromatography (Agilent 1200 Series, Santa Clara, CA, USA) coupled with a TSQ Quantum triple quadrupole mass spectrometer (Thermo-Electron, San Jose, CA, USA), as previously described [33]. The lower limit of quantitation was 1 ng ml^{-1}. The total assay variability (%CV) was 6.6% and 10.5% for doxorubicin and doxo'ol, respectively, and accuracy was 102% and 103%, respectively. Plasma NT-proBNP and troponin were measured before and at 4 h, 24 h and 48 h after doxorubicin infusion (Fairview Diagnostic Laboratories, St Paul, MN, USA).

Population PK and PD analysis

Population PK and PK-PD analysis of doxorubicin, doxo'ol and NT-proBNP were performed by means of nonlinear mixed-effects modelling using NONMEM 7.2 (ICON Development solution, Ellicott City, MD, USA). The first-order conditional estimation with interaction method (FOCE-INTERACTION) was used for the analysis. Model selection between competing nested models was performed by the likelihood ratio test as well as examination of diagnostics plots, which were generated by the Xpose package (version 4.0, Uppsala University, Uppsala, Sweden) using R (version 3.1.2, R Foundation, Vienna, Austria).

PK structural model

The schematic representation of the PK model for doxorubicin and doxo'ol is presented in Figure 1A. Initially, one-, two- and three-compartment structural disposition models were tested using plasma doxorubicin concentrations. The $PRIOR subroutine was used to incorporate *a priori* doxorubicin PK information [34] (Table S1). In the next step, the model for doxo'ol plasma concentrations was developed using a sequential model-building approach [35, 36], where doxorubicin PK parameters were fixed to the empirical Bayes estimates obtained from the previous step. As not all doxo'ol
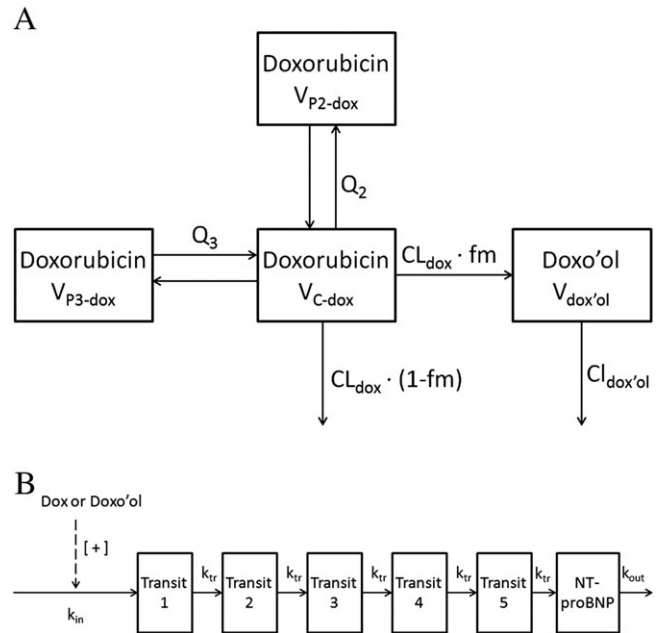

Figure 1

Pharmacokinetic and pharmacodynamic structural models. A. Pharmacokinetic model for doxorubicin (dox) and doxorubicinol (doxo'ol). CL_{dox} and $CL_{doxo'ol}$, elimination clearance of dox and doxo'ol, respectively; fm, fraction metabolized to doxo'ol; Q_2 and Q_3, intercompartmental clearances of doxorubicin; V_{C-dox}, V_{P2-dox} and V_{P3-dox}, the volume of distribution of doxorubicin for central and two peripheral compartments, respectively; $V_{doxo'ol}$, the volume of distribution of doxo'ol. B. Pharmacodynamic model of doxorubicin-induced N-terminal pro-brain natriuretic peptide (NT-proBNP) production. [+]: stimulatory effect; dox, doxorubicin; doxo'ol, doxorubicinol; k_{in}, production rate of the first step in NT-proBNP synthesis pathway; k_{out}, degradation rate constant of NT-proBNP synthesis pathway; k_{tr}, transit rate constant; NT-proBNP, NT-proBNP compartment; Transit 1–5, transit compartment 1–5

PK parameters, namely fraction metabolized to doxo'ol (fm), clearance ($CL_{doxo'ol}$) and volume of distribution ($V_{doxo'ol}$), are uniquely identifiable with plasma data only, the model was reparameterized so that $CL_{doxo'ol}/fm$ and $V_{doxo'ol}/fm$ were estimated.

PK-PD structural model

A population PK-PD model was developed to characterize the relationship between plasma doxorubicin and doxo'ol, and plasma NT-proBNP concentrations as a PD response variable. The model was developed using a sequential model-building approach [35, 36]. The individual PK parameter estimates obtained from the previous population PK modelling step were used to generate predicted individual doxorubicin concentrations for the population PK-PD analysis. For the NT-proBNP response, an indirect model with five transit compartments, as illustrated in Figure 1B, adequately described the PK-PD relationship: k_{in} represents the zero-order production rate of the first step in the NT-proBNP production pathway, and k_{tr} represents the first-order elimination rate constant of each transit compartment. The first-order degradation rate constant of NT-proBNP is represented by k_{out}, which was fixed

to 1.66 according to the previously estimated half-life of NT-proBNP [37]. The effect of doxorubicin (Effect) is assumed to increase k_{in} (Equation (1)), where k_{in_0} represents the baseline production rate.

$$k_{in} = k_{in\_0} \cdot (1 + Effect) \tag{1}$$

The mean transit time (MTT), which is expressed in Equation (2), represents the delay between drug exposure and response measured as change in NT-proBNP concentration.

$$MTT = \frac{number\ of\ transit\ compartments}{k_{tr}} \tag{2}$$

The effect of drug exposure was modelled using either a linear (Equation (3)) or an Emax (maximum response achievable; Equation (4)) relationship:

$$Effect = \beta \cdot C_{dox} \tag{3}$$

$$Effect = \frac{Emax \cdot C_{dox}}{EC50 + C_{dox}} \tag{4}$$

C_{dox} is the predicted plasma doxorubicin concentration. We also tested the effect of doxo'ol by using its predicted plasma concentration instead of C_{dox} in the above equations.

Random-effect model

The between-subject variability (BSV) on the PK and PK-PD parameters was modelled according to log-normal distribution as described as:

$$P_i = TVP \cdot \exp(\eta_i) \tag{5}$$

where P_i is the parameter estimate for the ith individual, TVP is the typical value of the parameter P and η_i is a random variable, which accounts for the interindividual difference between P_i and TVP. The values of η_i were assumed to come from a normal distribution, with mean of zero and variance ω^2. BSV was tested on all parameters in the model and included in the next model-building step if the improvement in the objective function value was significant at the 0.05 significance level. Correlations between individual parameter estimates were also examined. Interoccasion variability (IOV) was tested on PK and PK-PD parameters after the structural and covariate models had been established and included in the model if significant at the 0.05 significance level. Proportional, additive and combined error models were tested to describe residual unexplained variability (RUV). Shrinkage of random-effect variables was calculated for the final model [38].

Covariate model

Covariates (patient clinical factors, listed in Table 1) of interest were first selected based on the physiological and biological plausibility to influence the doxorubicin and doxo'ol PK, and NT-proBNP response. Creatinine clearance was estimated using the Cockroft–Gault equation. In addition to the covariates listed in Table 1, the following covariates were tested for

Table 1

Patient characteristics

Patient characteristics	Median (Range)
Age (years)	45(28–58)
Weight (kg)	65.3(54.5–140.4)
Height (m)	1.63(1.52–1.88)
BMI (kg m^{-2})	25.3(21.5–53.0)
BSA (m^{-2})	1.71(1.60–2.50)
Serum creatinine (mg dl^{-1})	0.7 (0.5–1.0)
Creatinine clearance (ml min^{-1})	121.90 (69.15–167.70)
AST (IU l^{-1})	26.0 (18.0–33.0)
ALT (IU l^{-1})	28.0 (8.0–62.0)
Total bilirubin (mg dl^{-1})	0.5 (0.2–1.0)
Baseline LVEF (%)	60 (48–69)

ALT, alanine aminotransferase; AST, aspartate transaminase; BMI, body mass index; BSA, body surface area; LVEF, left ventricular ejection fraction.

their influence on the parameters of the PK-PD relationship: cumulative dose of doxorubicin and the use of enalapril. Others have reported effects of enalapril on NT-proBNP concentrations [39]; therefore, we hypothesized that this covariate would be associated with NT-proBNP within-patient variability in our crossover study (on and off enalapril).

The above covariates were inspected visually for their correlation with PK or PD parameters using scatter plots. Collinearity among covariates was then assessed by Spearman rank coefficient of covariate–covariate correlations. If the corresponding Spearman rank correlation coefficient between two covariates was ≥0.5, one of the two covariates was removed. In the case of missing covariate values (one patient missing the baseline left ventricular ejection fraction, and one patient missing alanine aminotransferase, serum creatinine and creatinine clearance values), the median population value was used for that individual. After this step, the following covariates remained of interest: age, height, body surface area (BSA), total bilirubin, and creatinine clearance, all of which are continuous variables. Finally, the remaining covariates were tested in NONMEM using a stepwise covariate model (SCM)-building strategy. Covariates were considered to be significant if their inclusion in a nested model resulted in an objective function value (OFV) drop of 3.84 or more (chi-square, df = 1, $P < 0.05$) and their exclusion from the full model resulted in an OFV rise of 6.63 (chi-square, df = 1, $P < 0.01$) or more. The effect of a continuous covariate (e.g. BSA, creatinine clearance) on a parameter was estimated relative to the median covariate value in the data set using a power function model (Equation (6)).

$$TVP = \theta_1 * \left(\frac{Cov}{Median_{cov}} \right) ** \theta_2 \tag{6}$$

The use of enalapril was the only categorical covariate that was evaluated. Its effect on a parameter was estimated using Equation (7), where ENAL = 1 for on and 0 for off enalapril.

$$TVP = \theta_1 * \theta_2 ** ENAL \tag{7}$$

Model evaluation

The population models for doxorubicin PK, doxo'ol PK and doxorubicin NT-proBNP PK-PD were evaluated separately with visual predictive checks and nonparametric bootstrap analysis. For the predictive check, 1000 data sets were simulated from each model using the final model parameters. The median, 5th and 95th percentiles of the simulated concentrations were calculated and compared with the observed data. For the bootstrap analysis, 1000 bootstrap runs were performed. The final model developed from the original data set was fitted to each of the bootstrap data sets to obtain the bootstrap parameter estimates. The median, 2.5th and 97.5th percentiles of the parameter estimates were computed from the bootstrap runs and compared with the point estimates results from the original data set.

Result

Patients

A total of 236 doxorubicin concentrations and 237 doxo'ol concentrations from 17 patients were used in model development. Patients received 60 mg m^{-2} doxorubicin (intended dose, actual range 54–65 mg m^{-2}) per cycle, which was infused for 15 min (intended infusion time, actual range 5–60 min). By the time of enrolment in the current study, one patient had not previously received any cycle of doxorubicin, and three and 13 patients had received one and two cycles of doxorubicin, respectively. Patient characteristics are summarized in Table 1.

PK of doxorubicin and doxo'ol

The doxorubicin plasma concentrations were fitted using one-, two- or three-compartment models. Initially, while diagnostic plots of the two-compartment models indicated model misspecification, the three-compartment model was unstable and with large estimate imprecision (data not shown). Previously published information on doxorubicin PK [34] was incorporated to stabilize the three-compartment model by using the $PRIOR subroutine. The resulting model (Figure 1A) adequately described the doxorubicin concentration–time profile. It allowed estimation of BSV associated with CL_{dox}, $V_{C\text{-}dox}$, $Q_{2\text{-}dox}$ and $V_{2\text{-}dox}$, and IOV associated with CL_{dox}. Residual unexplained variability was best described using a combined additive and proportional error model. Covariates were not observed to be associated with doxorubicin PK variability. Parameter estimates from the best-fitted model are shown in Table 2, and the goodness-of-fit plots are presented in Figures 2A and B.

The PK of doxorubicin's OH-metabolite, doxo'ol, was best described by a one-compartment model (Figure 1A). The model allowed estimation of BSV associated with clearance ($CL_{doxo'ol}$/fm) and volume of distribution ($V_{doxo'ol}$/fm), and IOV associated with $CL_{doxo'ol}$/fm and $V_{doxo'ol}$/fm. Residual unexplained variability was best described using a proportional error model. Similar to doxorubicin, covariates were not observed to be significantly associated with doxo'ol PK variability. The parameter estimates of doxo'ol model are shown in Table 2, and goodness-of-fit plots from the final model in Figures 2C and D. While

doxo'ol concentrations >25 ng ml^{-1} were underpredicted from the model (Figure 2C), neither adding an additional metabolite compartment nor log-transformation of the data improved model fit (Figure S2).

The population PK-PD model of doxorubicin-induced acute cardiotoxicity response

During the 48 h following the doxorubicin infusion, NT-proBNP concentrations at 4 h after infusion did not differ from baseline, but increased at 24 h and 48 h (Figure 3C). By contrast, troponin concentrations remained unchanged (mean 0.014 ng ml^{-1}, range 0.012–0.048, data not shown) over the entire period. Therefore, a PD model was developed with NT-proBNP as response variable.

For PK-PD modelling, an indirect model with five transit compartments (Figure 1B) provided a satisfactory characterization of the PK-PD relationship between doxorubicin PK and plasma NT-proBNP concentrations. As illustrated in Figure 1B, the model assumes that doxorubicin stimulated NT-proBNP production. The typical value of the baseline production rate (K_{in_0}) of NT-proBNP was estimated to be 97.4 ng·ml^{-1}·h^{-1}. The typical value of mean transit time (MTT, Equation (2)), which represents the delay between doxorubicin exposure and response measured as change in NT-proBNP concentration was estimated to be 34.7 h. Four or six transit compartments were also used to fit the model instead of five (data not shown). This led to a minimal change in estimated PD parameters and a nonsignificant change in OFV. The stimulatory effect of doxorubicin was modelled using a linear relationship (Equation (3)) as the Emax relationship (Equation (4)) resulted in overparameterization. The PK-PD model was also tested, assuming that doxo'ol stimulates NT-proBNP production. This resulted in little change in OFV or goodness-of-fit plots (data not shown). The estimated PD parameters are presented in Table 3, and goodness-of-fit plots are shown in Figures 2E and F. A large BSV (40–70%) was found in PD parameters. No tested covariates were associated with PD variability.

Model evaluation

The predictive check plots of doxorubicin, doxo'ol and NT-proBNP are depicted in Figure 3. No systematic deviation was observed between the observed and simulated data.

From 1000 bootstrap runs for each model, 776, 801 and 720 runs of doxorubicin, doxo'ol and NT-proBNP, respectively, had a successful minimization and were included in the bootstrap analysis. Tables 2, 3 show the parameter estimates and relative standard error obtained from the final model compared with parameter estimates and nonparametric 95% CIs obtained from the bootstrap approach. The median parameter estimates for the fixed and random effects from the bootstrap approach were comparable to those obtained from the final model. The point estimates obtained from the original data set showed close agreement with the median and were all included within the 2.5th to the 97.5th percentiles of the bootstrapping values, indicating model stability.

Table 2

Parameter estimates for doxorubicin and doxorubicinol pharmacokinetic model

Parameter (unit)	Estimate (RSE) [Shrinkage]	Bootstrap median [95% CI]
CL_{dox} ($l\,h^{-1}$)	54.2 (2%)	54.1 [52.2, 55.8]
$V_{C\text{-}dox}$ (l)	16.9 (2%)	16.8 [16.0, 17.5]
$Q_{2\text{-}dox}$ ($l\,h^{-1}$)	66.1 (3%)	66.3 [63.5, 69.5]
$V_{2\text{-}dox}$ (l)	1650 (3%)	1648 [1547, 1741]
$Q_{3\text{-}dox}$ ($l\,h^{-1}$)	23.4 (4%)	23.3 [21.4, 25.1]
$V_{3\text{-}dox}$ (l)	61.8 (6%)	61.6 [54.7, 69.6]
BSV		
BSV-CL_{dox} (% CV)	8.33 (33%)[19%]	8.01 [2.51, 12.9]
BSV-$V_{C\text{-}dox}$ (% CV)	10.5 (33%)[26%]	10.5 [2.98, 16.7]
BSV-$Q_{2\text{-}dox}$ (% CV)	15.4 (20%)[10%]	14.8 [8.89, 21.5]
BSV-$V_{2\text{-}dox}$ (% CV)	26.7 (18%)[11%]	25.8 [13.4, 35.4]
IOV		
IOV-$CL_{C\text{-}dox}$ (% CV)	3.86 (29%)[42%]	3.93 [1.67, 6.13]
RUV		
RUV-proportional-dox (% CV)	8.73 (9.8%) [13%]	8.47 (6.88, 9.99)
RUV-additive-dox (SD)	0.60 (41%) [13%]	0.52 (0.034, 1.79)
$CL_{doxo'ol}/fm$ ($l\,h^{-1}$)	106 (5%)	105 [95–116]
$V_{C\text{-}doxo'ol}/fm$ (l)	1880 (9%)	1876 [1582–2205]
BSV		
BSV-$CL_{doxo'ol}/fm$ (% CV)	18.5 (30%) [10%]	17.8 [5–18]
BSV-$V_{doxo'ol}/fm$ (% CV)	37.3 (15%) [0%]	35.7 [24.7–48.0]
IOV		
IOV-$CL_{doxo'ol}/fm$ (% CV)	11.9 (43%) [49%]	11.4 [2.3–19.6]
IOV-$V_{doxo'ol}/fm$ (% CV)	9.39 (26%) [47%]	8.72 [2.64–13.3]
RUV		
RUV-proportional-doxo'ol (% CV)	14.9 (12%) [12%]	14.6 [11.4–18.4]

BSV was calculated from $\sqrt{\exp\,(\omega^2 - 1)}$ and expressed as the CV%. Proportional RUV is expressed as CV%, and additive RUV as SD. RSE is expressed as CV% (RSE of BSV, IOV and RUV is expressed in term of SD). Shrinkage of BSV, IOV and RUV is presented in square brackets. CI, confidence interval; BSV, between-subject variability; CV%, coefficient of variation; dox, doxorubicin; doxo'ol, doxorubicinol; IOV, interoccasion variability; RSE, relative standard error; RUV, random unexplained variability; SD, standard deviation.

Discussion

Anthracyclines rank among the most effective anticancer drugs. However, their clinical usefulness is hampered by the risk of cardiotoxicity. Clinically, anthracycline-induced cardiotoxicity is monitored by left ventricular ejection fraction (LVEF) assessment. However, the cardiac side effect of anthracyclines can take months or years to progress, and decreased LVEF is not observed until irreversible myocardial damage has occurred. Earlier studies suggested that acute responses may be indicative of long-term anthracycline toxicity [26, 27]. Therefore, understanding detectable acute cardiac response after anthracycline exposure may provide a useful insight for patients who could experience subsequent anthracycline cardiotoxicity.

The development of population PK models for doxorubicin and doxo'ol have been reported in previous studies [34, 40–42]. Doxorubicin is typically described by a three-compartment model. In the current study, although the observed concentration–time profile of doxorubicin exhibited triexponential features, a three-compartment model was not stable. $PRIOR function was used to stabilize the structure model with *a priori* information from Kontny *et al.* [34]. For the PK of doxo'ol, a one-compartment model was used. The disposition of doxo'ol is known to be formation rate limited [43]. Parameter estimates of doxo'ol were consistent with those in previous reports [34, 40–42]. Sequential and simultaneous fitting of the parent–metabolite data gave consistent results. In the current study, BSV in doxorubicin and doxo'ol PK parameters ranged from 10% to 40%, which is consistent with previous reports (10–50%) [34, 40–42]. Some, but not all, earlier studies reported BSA, aspartate transaminase, age, creatinine clearance [42] and body mass index [41] as significant covariates for doxorubicin and/or doxo'ol PK parameter variability. No significant relationship was found between patient-specific characteristics and PK variability in the present study, which may have been due to the small sample size and the relative homogeneity of the study participants.

In the present study, we sought to understand and characterize the acute changes in plasma NT-proBNP concentrations in response to doxorubicin treatment, which then may provide a method to identify patients at high risk for
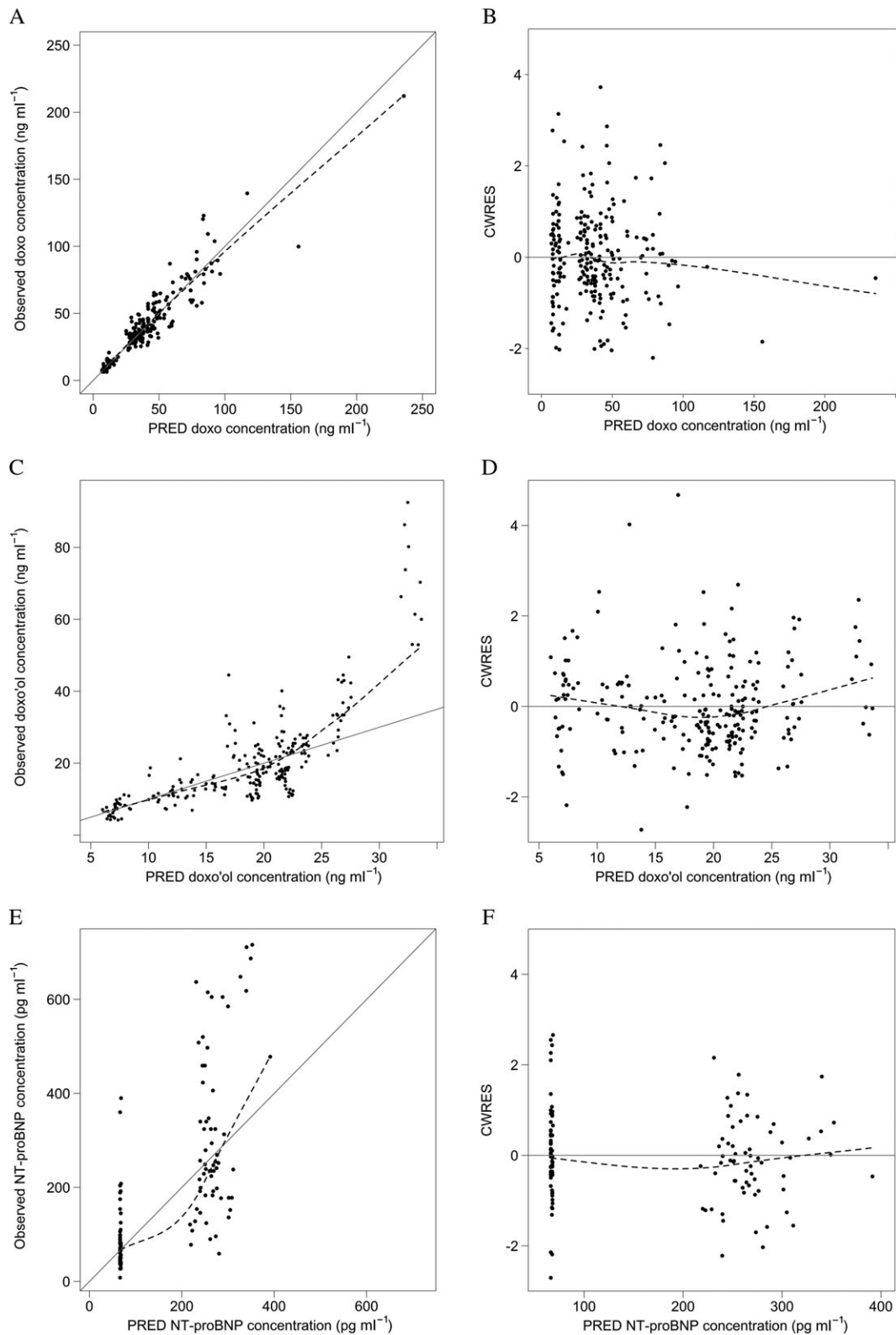
Figure 2
Goodness-of-fit plots for the population pharmacokinetic models of doxorubicin (doxo) and doxorubicinol (doxo'ol), and the pharmacodynamic model of dox-induced N-terminal pro-brain natriuretic peptide (NT-proBNP) production. Identity plot of observed *vs.* population-predicted (PRED) concentrations of doxo (A), doxo'ol (C) and NT-proBNP (E). Scatter plot of conditional weighted residuals (CWRES) *vs.* PRED concentration of doxo (B), doxo'ol (D) and NT-proBNP (F). Points represent the observations; dashed line shows smoothed (loess) line through the data; the solid line shows the line of identity in panels A, C and E
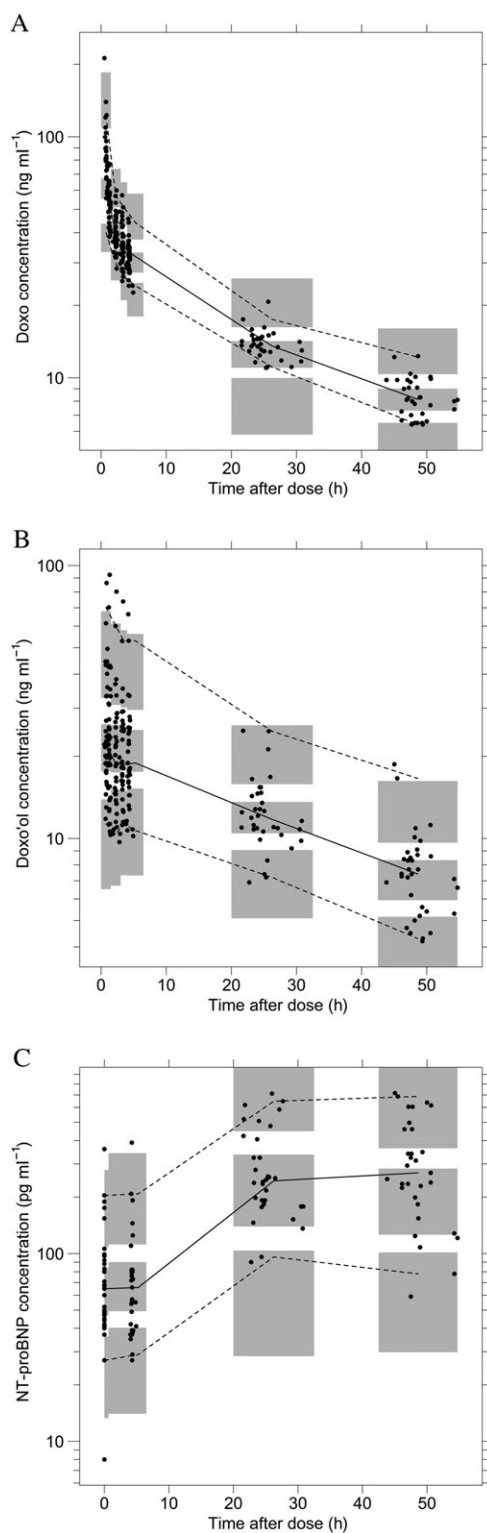
A

B

C

Figure 3

Visual predictive check plots for the pharmacokinetic model of doxo-rubicin (doxo) (A) and doxorubicinol (doxo'ol) (B), and the PK-PD model of N-terminal pro-brain natriuretic peptide (NT-proBNP) (C). Circles represent observations. Lines represent 5th (dashed), 50th (solid) and 95th (dashed) percentiles of observations; and shaded areas represent the 95% confidence intervals of the 5th, 50th and 95th quantiles of the simulated data sets from the model

Table 3

Parameter estimate for the pharmacodynamic model of NT-proBNP

Parameter (unit)	Estimate (RSE) [Shrinkage]	Bootstrap median [95% CI]
k_{in_o} (ng·ml^{-1} h^{-1})	110 (13%)	102 (73, 144)
k_{out} (h^{-1})*	1.66 (−)	−
β (l·μg^{-1})	115 (22%)	98 (47, 166)
MTT (h)	34.7 (12%)	42 (30, 52)
BSV		
BSV-k_{in_o} (% CV)	48.5 (22%) [8%]	51.6 (11.8, 87.1)
BSV-β (% CV)	73.9 (21%) [8%]	83.5 (37.0, 144)
BSV-MTT (% CV)	38.8 (34%) [8%]	34.8 (2.4, 61.1)
IOV		
IOV-k_{in_o} (% CV)	27.8 (17%) [27%]	26.9 (18.4, 38.6)
RUV		
RUV-BNP (% CV)	23.8 (15.2%) [23%]	23.6 (17.0, 32.3)

*this parameter was fixed to literature value. β, slope factor as defined in Equation (3). BSV, between-subject variability; CI, confidence interval; CV%, coefficient of variation; IOV, interoccasion variability; k_{in_o}, baseline production rate of NT-proBNP; k_{out}, degradation rate constant of NT-proBNP synthesis pathway; MTT, mean transit time; NT-proBNP, N-terminal pro B-type natriuretic peptide; RUV, random unexplained variability;. Shrinkage of BSV, IOV and RUV is presented in square brackets.

later cardiac impairment. A population PK-PD model was developed to describe the acute NT-proBNP response after doxorubicin infusion. To the best of our knowledge, this is the first report of the development of a PK-PD model for anthracycline-induced NT-proBNP production. As the acute response of NT-proBNP following anthracycline exposure is a dynamic process, a PK-PD model provides a better description of this process than using a single summary statistic (i.e. maximal observed NT-proBNP concentration). In the PK-PD model developed here (Figure 1B), NT-proBNP production and elimination are represented by the rate of k_{in} and rate constant k_{out}. The effect of doxorubicin in stimulating NT-proBNP production (Effect$_{dox}$) is expressed as proportional to the individual model-predicted plasma doxorubicin (C_{dox}). The molecular pathway of NT-proBNP expression and secretion is mimicked by the chain of transit compartments (Transit 1–5) with the mean transit time MTT, which represents the delay between drug exposure and the NT-proBNP response. It should be noted that the PK-PD model developed here is greatly limited by PD sampling time points. As a result, we had to fix the degradation rate constant of NT-proBNP according to the previously estimated half-life of NT-proBNP [37] in order to obtain a stable model. We were also unable to differentiate between models with different numbers of transit compartments. Simulation using model-estimated typical parameter values (Figure S3) shows that plasma NT-proBNP will gradually increase from 4 h to 35 h and decrease afterwards. While the model adequately described the observed data, sampling at additional time points would help to further improve the model. In an early study by Sandri *et al.* [32], the acute NT-proBNP response was categorized into three patterns: no change, a transient increase followed by a return to baseline at 72 h, or a persistent increase. In the current study,
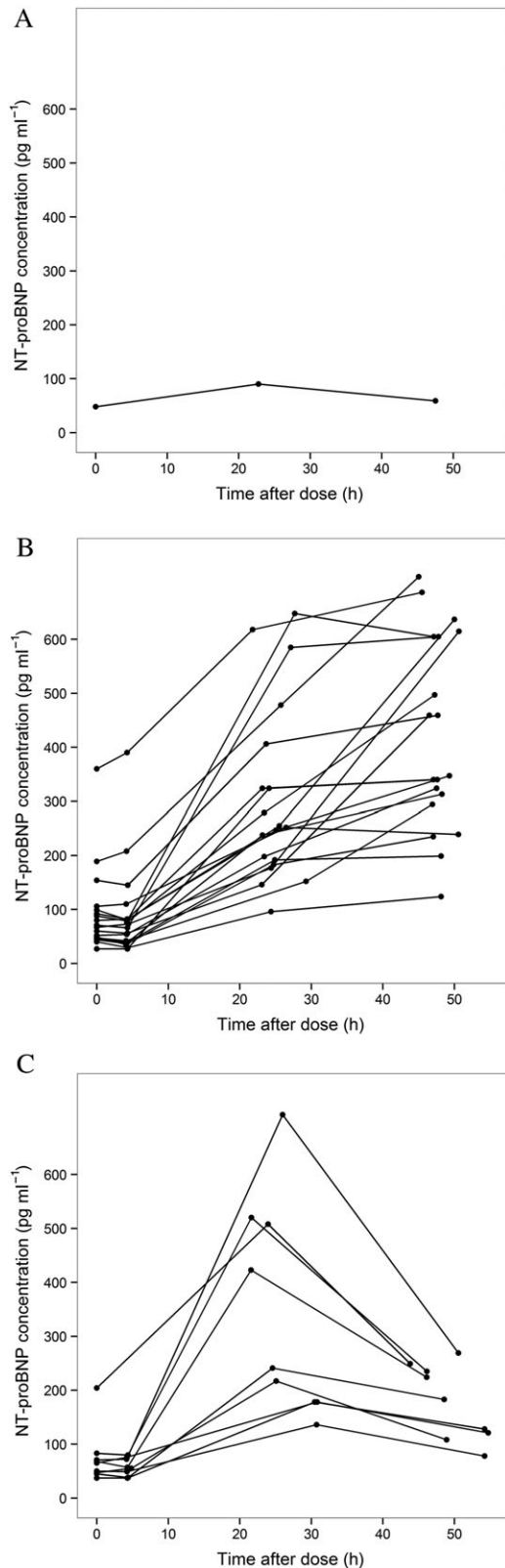
Figure 4

N-terminal pro-brain natriuretic peptide (NT-proBNP) concentrations at different sampling times. Three different patterns of NT-proBNP response were observed: minimal change (A), increase at 24 h and decrease at 48 h (B) and persistent increase (C)

we observed similar patterns. We grouped NT-proBNP responses into three types of pattern, based on visual inspection (Figure 4). The PK-PD model we developed was able to capture these types of NT-proBNP responses in the current data set; however, greater accuracy in prediction is needed due to high BSV.

High BSV (38.8–73.9%, Table 3) was observed for PD parameters. Covariates were not found to be associated with PD variability, which is probably because of the limited sample size in the current study. To our knowledge, covariate(s) associated with NT-proBNP variability in patients with breast cancer receiving doxorubicin have not been reported. In other patient populations, polymorphisms in the BNP gene and type A human natriuretic peptide receptor gene, cigarette smoking, body mass index, age and blood pressure have been associated with NT-proBNP variability [44–47]. Our model would therefore be expected to provide a valuable framework for future studies to identify clinical factors associated with the acute response to doxorubicin.

The effect of coadministration of enalapril was tested on PD parameters and found to be nonsignificant. While the effectiveness of angiotensin antagonists in preventing anthracycline-induced long-term cardiotoxicity has been demonstrated by several small clinical trials [48–50], the effect on the immediate cardiac biomarker response to anthracycline has not been reported. In one clinical trial in patients with systolic heart failure [39], investigators tested for the effect of enalapril administration on plasma NT-proBNP concentrations. After 6 months of continuous therapy, they observed a 34% decrease in NT-proBNP in the enalapril-treated group relative to controls. In the present shorter-duration study in patients with breast cancer, we did not observe a covariate effect for enalapril on acute NT-proBNP concentrations. Further, the NT-proBNP concentrations that we report are similar to those reported by Romano *et al.* [31] and Sandri *et al.* [32]. It should be noted that 16 out of the 17 study participants had received at least one cycle of doxorubicin treatment prior to the enrolment in the current study. It is possible that the effect of enalapril would have been more notable if it had been given before the first dose of chemotherapy.

In addition to NT-proBNP, another commonly used cardiotoxicity biomarker, troponin, was also quantified. In contrast to NT-proBNP, the concentration of troponin did not change within 48 h following the doxorubicin infusion, which was similar to the results of Romano *et al.* [31], who also reported an increase in NT-proBNP but not troponin concentration in most patients. Troponin is a structural protein of the myocardium, and an increased troponin concentration is considered to be a specific marker of myocardial damage. The difference between levels of NT-proBNP and troponin following doxorubicin infusion could suggest that the acute toxicity of low-to-medium doxorubicin exposure mainly results in a decreased contractile reserve, but not myocardial damage.

In conclusion, the PK-PD relationship of doxorubicin and the acute NT-proBNP response was best described by a turnover model with five transit compartments. The typical value of mean transit time was estimated to be 34.7 h, which represents the delay between doxorubicin exposure and the change in the NT-proBNP concentration. High BSV was observed in PD parameters. This model can be used in future studies to test important patient-specific characteristics that influence PD variability, and susceptibility to later cardiac symptoms.

Competing Interest

References

1 Lopez M, Vici P, Di Lauro K, Conti F, Paoletti G, Ferraironi A, *et al*. Randomized prospective clinical trial of high-dose epirubicin and dexrazoxane in patients with advanced breast cancer and soft tissue sarcomas. J Clin Oncol 1998; 16: 86–92.

2 Moore S. Drug-induced congestive heart failure in breast cancer survivors. Clin Excell Nurse Pract 2001; 5: 129–33.

3 Slamon DJ, Leyland-Jones B, Shak S, Fuchs H, Paton V, Bajamonde A, *et al*. Use of chemotherapy plus a monoclonal antibody against HER2 for metastatic breast cancer that overexpresses HER2. N Engl J Med 2001; 344: 783–92.

4 Minotti G, Menna P, Salvatorelli E, Cairo G, Gianni L. Anthracyclines: molecular advances and pharmacologic developments in antitumor activity and cardiotoxicity. Pharmacol Rev 2004; 56: 185–229.

5 Schlitt A, Jordan K, Vordermark D, Schwamborn J, Langer T, Thomssen C. Cardiotoxicity and oncological treatments. Dtsch Arztebl Int 2014; 111: 161–8.

6 Carvalho FS, Burgeiro A, Garcia R, Moreno AJ, Carvalho RA, Oliveira PJ. Doxorubicin-induced cardiotoxicity: from bioenergetic failure and cell death to cardiomyopathy. Med Res Rev 2014; 34: 106–35.

7 Octavia Y, Tocchetti CG, Gabrielson KL, Janssens S, Crijns HJ, Moens AL. Doxorubicin-induced cardiomyopathy: from molecular mechanisms to therapeutic strategies. J Mol Cell Cardiol 2012; 52: 1213–25.

8 Sterba M, Popelova O, Vavrova A, Jirkovsky E, Kovarikova P, Gersl V, *et al*. Oxidative stress, redox signaling, and metal chelation in anthracycline cardiotoxicity and pharmacological cardioprotection. Antioxid Redox Signal 2013; 18: 899–929.

9 Nitiss KC, Nitiss JL. Twisting and ironing: doxorubicin cardiotoxicity by mitochondrial DNA damage. Clin Cancer Res 2014; 20: 4737–9.

10 Boucek RJ Jr, Miracle A, Anderson M, Engelman R, Atkinson J, Dodd DA. Persistent effects of doxorubicin on cardiac gene expression. J Mol Cell Cardiol 1999; 31: 1435–46.

11 Sishi BJ, Bester DJ, Wergeland A, Loos B, Jonassen AK, van Rooyen J, *et al*. Daunorubicin therapy is associated with upregulation of E3 ubiquitin ligases in the heart. Exp Biol Med (Maywood) 2012; 237: 219–26.

12 Lebrecht D, Setzer B, Rohrbach R, Walker UA. Mitochondrial DNA and its respiratory chain products are defective in doxorubicin nephrosis. Nephrol Dial Transplant 2004; 19: 329–36.

13 Lyu YL, Kerrigan JE, Lin CP, Azarova AM, Tsai YC, Ban Y, *et al*. Topoisomerase IIbeta mediated DNA double-strand breaks: implications in doxorubicin cardiotoxicity and prevention by dexrazoxane. Cancer Res 2007; 67: 8839–46.

14 Khiati S, Dalla Rosa I, Sourbier C, Ma X, Rao VA, Neckers LM, *et al*. Mitochondrial topoisomerase I (top1mt) is a novel limiting factor of doxorubicin cardiotoxicity. Clin Cancer Res 2014; 20: 4873–81.

15 Forrest GL, Akman S, Doroshow J, Rivera H, Kaplan WD. Genomic sequence and expression of a cloned human carbonyl reductase gene with daunorubicin reductase activity. Mol Pharmacol 1991; 40: 502–7.

16 Torres VM, Simic VD. Doxorubicin-Induced Oxidative Injury of Cardiomyocytes – Do We Have Right Strategies for Prevention? In: InTech, ed Fiuza M, 2012. DOI: 10.5772/34692. Available from: http://www.intechopen.com/books/cardiotoxicity-of-oncologic-treatments/doxorubicin-induced-oxidative-injury-of-cardiomyocytes-do-we-have-right-strategies-for-prevention-

17 Singal PK, Iliskovic N. Doxorubicin-induced cardiomyopathy. N Engl J Med 1998; 339: 900–5.

18 Christiansen S, Autschbach R. Doxorubicin in experimental and clinical heart failure. Eur J Cardiothorac Surg 2006; 30: 611–6.

19 Yeh ET, Bickford CL. Cardiovascular complications of cancer therapy: incidence, pathogenesis, diagnosis, and management. J Am Coll Cardiol 2009; 53: 2231–47.

20 Buzdar AU, Marcus C, Smith TL, Blumenschein GR. Early and delayed clinical cardiotoxicity of doxorubicin. Cancer 1985; 55: 2761–5.

21 Jain D. Cardiotoxicity of doxorubicin and other anthracycline derivatives. J Nucl Cardiol 2000; 7: 53–62.

22 Blaes A, Duprez D, Defor T, Shanley R, Beckwith H, Haddad T, *et al*. Angiotensin converting enzyme inhibitors (ACEI) and doxorubicin pharmacokinetics in women receiving adjuvant breast cancer treatment. Springerplus 2015; 4: 32.

23 Monti M, Terzuoli E, Ziche M, Morbidelli L. The sulphydryl containing ACE inhibitor zofenoprilat protects coronary endothelium from doxorubicin-induced apoptosis. Pharmacol Res 2013; 76: 171–81.

24 Lipshultz SE, Rifai N, Sallan SE, Lipsitz SR, Dalton V, Sacks DB, *et al*. Predictive value of cardiac troponin T in pediatric patients at risk for myocardial injury. Circulation 1997; 96: 2641–8.

25 Mavinkurve-Groothuis AM, Kapusta L, Nir A, Groot-Loonen J. The role of biomarkers in the early detection of anthracycline-induced cardiotoxicity in children: a review of the literature. Pediatr Hematol Oncol 2008; 25: 655–64.

26 Herman EH, Zhang J, Lipshultz SE, Rifai N, Chadwick D, Takeda K, *et al*. Correlation between serum levels of cardiac troponin-T and the severity of the chronic cardiomyopathy induced by doxorubicin. J Clin Oncol 1999; 17: 2237–43.

27 Lipshultz SE, Rifai N, Dalton VM, Levy DE, Silverman LB, Lipsitz SR, *et al*. The effect of dexrazoxane on myocardial injury in doxorubicin-treated children with acute lymphoblastic leukemia. N Engl J Med 2004; 351: 145–53.

28 Tian S, Hirshfield KM, Jabbour SK, Toppmeyer D, Haffty BG, Khan AJ, *et al*. Serum biomarkers for the detection of cardiac toxicity after chemotherapy and radiation therapy in breast cancer patients. Front Oncol 2014; 4: 277.

29 Yancy CW, Jessup M, Bozkurt B, Butler J, Casey DE Jr, Drazner MH, *et al*. 2013 ACCF/AHA guideline for the management of heart failure: a report of the American College of Cardiology Foundation/American Heart Association Task Force on practice guidelines. Circulation 2013; 128: e240–327.

30 McMurray JJ, Adamopoulos S, Anker SD, Auricchio A, Bohm M, Dickstein K. ESC guidelines for the diagnosis and treatment of acute and chronic heart failure 2012: the Task Force for the Diagnosis and Treatment of Acute and Chronic Heart Failure 2012 of the European Society of Cardiology. Developed in collaboration with the Heart Failure Association (HFA) of the ESC. Eur Heart J 2012; 33: 1787–847.

31 Romano S, Fratini S, Ricevuto E, Procaccini V, Stifano G, Mancini M, et al. Serial measurements of NT-proBNP are predictive of not-high-dose anthracycline cardiotoxicity in breast cancer patients. Br J Cancer 2011; 105: 1663–8.

32 Sandri MT, Salvatici M, Cardinale D, Zorzino L, Passerini R, Lentati P, et al. N-terminal pro-B-type natriuretic peptide after high-dose chemotherapy: a marker predictive of cardiac dysfunction? Clin Chem 2005; 51: 1405–10.

33 DiFrancesco R, Griggs JJ, Donnelly J, DiCenzo R. Simultaneous analysis of cyclophosphamide, doxorubicin and doxorubicinol by liquid chromatography coupled to tandem mass spectrometry. J Chromatogr B Analyt Technol Biomed Life Sci 2007; 852: 545–53.

34 Kontny NE, Wurthwein G, Joachim B, Boddy AV, Krischke M, Fuhr U, et al. Population pharmacokinetics of doxorubicin: establishment of a NONMEM model for adults and children older than 3 years. Cancer Chemother Pharmacol 2013; 71: 749–63.

35 Zhang L, Beal SL, Sheiner LB. Simultaneous vs. sequential analysis for population PK/PD data I: best-case performance. J Pharmacokinet Pharmacodyn 2003; 30: 387–404.

36 Zhang L, Beal SL, Sheinerz LB. Simultaneous vs. sequential analysis for population PK/PD data II: robustness of methods. J Pharmacokinet Pharmacodyn 2003; 30: 405–16.

37 Kroll MH, Twomey PJ, Srisawasdi P. Using the single-compartment ratio model to calculate half-life, NT-proBNP as an example. Clin Chim Acta 2007; 380: 197–202.

38 Savic RM, Karlsson MO. Importance of shrinkage in empirical bayes estimates for diagnostics: problems and solutions. AAPS J 2009; 11: 558–69.

39 Rosenberg J, Gustafsson F, Remme WJ, Riegger GA, Hildebrandt PR. Effect of beta-blockade and ACE inhibition on B-type natriuretic peptides in stable patients with systolic heart failure. Cardiovasc Drugs Ther 2008; 22: 305–11.

40 Callies S, de Alwis DP, Wright JG, Sandler A, Burgess M, Aarons L. A population pharmacokinetic model for doxorubicin and doxorubicinol in the presence of a novel MDR modulator, zosuquidar trihydrochloride (LY335979). Cancer Chemother Pharmacol 2003; 51: 107–18.

41 Thompson PA, Rosner GL, Matthay KK, Moore TB, Bomgaars LR, Ellis KJ, et al. Impact of body composition on pharmacokinetics of doxorubicin in children: a Glaser Pediatric Research Network study. Cancer Chemother Pharmacol 2009; 64: 243–51.

42 Joerger M, Huitema AD, Richel DJ, Dittrich C, Pavlidis N, Briasoulis E, et al. Population pharmacokinetics and pharmacodynamics of doxorubicin and cyclophosphamide in breast cancer patients: a study by the EORTC-PAMM-NDDG. Clin Pharmacokinet 2007; 46: 1051–68.

43 Drug Label, Doxorubicin hydrochloride. FDA Drug Database, 2013 [online]. [cited 2015]. Available at http://www.accessdata.fda.gov/drugsatfda_docs/label/2013/050629s022lbl.pdf (last accessed May 2016).

44 Lajer M, Tarnow L, Jorsal A, Parving HH. Polymorphisms in the B-type natriuretic peptide (BNP) gene are associated with NT-proBNP levels but not with diabetic nephropathy or mortality in type 1 diabetic patients. Nephrol Dial Transplant 2007; 22: 3235–9.

45 Alyan O, Kacmaz F, Ozdemir O, Maden O, Topaloglu S, Ozbakir C, et al. Effects of cigarette smoking on heart rate variability and plasma N-terminal pro-B-type natriuretic peptide in healthy subjects: is there the relationship between both markers? Ann Noninvasive Electrocardiol 2008; 13: 137–44.

46 Fradley MG, Larson MG, Cheng S, McCabe E, Coglianese E, Shah RV, et al. Reference limits for N-terminal-pro-B-type natriuretic peptide in healthy individuals (from the Framingham Heart Study). Am J Cardiol 2011; 108: 1341–5.

47 Weber M, Burian M, Dragutinovic I, Moellmann H, Nef H, Elsaesser A, et al. Genetic polymorphism of the type A human natriuretic peptide receptor (NPR-A) gene contributes to the interindividual variability in the BNP system. Eur J Heart Fail 2008; 10: 482–9.

48 Bosch X, Rovira M, Sitges M, Domenech A, Ortiz-Perez JT, de Caralt TM, et al. Enalapril and carvedilol for preventing chemotherapy-induced left ventricular systolic dysfunction in patients with malignant hemopathies: the OVERCOME trial (preventiOn of left Ventricular dysfunction with Enalapril and caRvedilol in patients submitted to intensive ChemOtherapy for the treatment of Malignant hEmopathies). J Am Coll Cardiol 2013; 61: 2355–62.

49 Cardinale D, Colombo A, Sandri MT, Lamantia G, Colombo N, Civelli M, et al. Prevention of high-dose chemotherapy-induced cardiotoxicity in high-risk patients by angiotensin-converting enzyme inhibition. Circulation 2006; 114: 2474–81.

50 Nakamae H, Tsumura K, Terada Y, Nakane T, Nakamae M, Ohta K, et al. Notable effects of angiotensin II receptor blocker, valsartan, on acute cardiotoxic changes after standard chemotherapy with cyclophosphamide, doxorubicin, vincristine, and prednisolone. Cancer 2005; 104: 2492–8.

Supporting Information

Additional Supporting Information may be found in the online version of this article at the publisher's web-site:

http://onlinelibrary.wiley.com/doi/10.1111/bcp.12989/suppinfo.

Figure S1 Scatter plot of conditional weighted residuals (CWRES) *vs.* time of the doxorubicin (A), doxorubicinol (B) and N-terminal pro-brain natriuretic peptide (C) model. Points represent the observations; dashed line shows smoothed (loess) line through the data

Figure S2 Scatter plot of conditional weighted residuals (CWRES) *vs.* population-predicted (PRED) concentration of doxorubicinol (D) using a two-compartment metabolite model (A) or log-transformed data (B). Points represent the observations; dashed line shows smoothed (loess) line through the data; the solid line shows the line of identity in panel

Figure S3 Model-predicted N-terminal pro-brain natriuretic peptides concentration 0–50 h following the doxorubicin infusion

Table S1 Parameter estimate and relative standard error used in the $PRIOR subroutine (from Kontny *et al.* [34]).